THE JOURNAL OF PHYSICAL CHEMISTRY C

Article

pubs.acs.org/JPCC

Reactive Ensemble Monte Carlo Simulations of Silica Polymerization That Yield Zeolites and Related Crystalline Microporous Structures

Szu-Chia Chien,[†] Scott M. Auerbach,*[,‡] and Peter A. Monson*[,†]

[†]Department of Chemical Engineering and [‡]Department of Chemistry, University of Massachusetts Amherst, Amherst, Massachusetts 01003, United States

Supporting Information

ABSTRACT: We have performed replica-exchange reaction ensemble Monte Carlo simulations to study the low-energy crystalline structures of a reactive model of silica. We have utilized a model of silica polymerization based on the reactive assembly of semiflexible tetrahedral units developed by us previously to reproduce silica bulk moduli as well as self-assembly of amorphous silica gels and nanoparticles. Our implementation of replica-exchange Monte Carlo involves simulating several system copies, each with its own value of the equilibrium constant controlling silica condensation/hydrolysis reactions, which are essential for building higher-order network structures and eventually crystals. These replica-exchange simulations were found to traverse energy landscapes from amorphous to crystalline phases, yielding the dense silica polymorphs α-cristobalite, β-cristobalite, and keatite, as well as the nanoporous silica materials SOD and EDI and nanoporous phosphates with DFT and ATT structures. Simulated crystal structures were confirmed by computing X-ray patterns for comparison with known XRD data. The behavior of this model opens the door to future simulation studies of the free energy barriers controlling these crystallization processes.

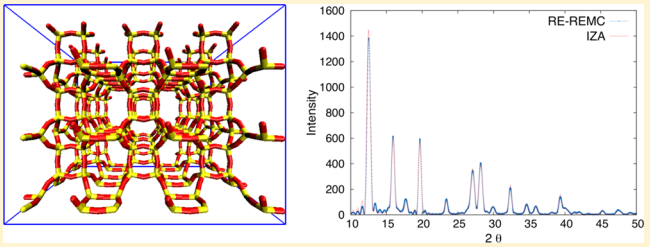

INTRODUCTION

Nanoporous materials such as zeolites are of great importance to chemical industries because of wide applications in catalysis and separations.[1−4] The development of new applications in areas such as drug delivery, shape-selective sensors, and nanoelectronic depends on tailoring material properties such as pore sizes, crystallite size and shape, and crystallite surface structures.[5−7] The ability of synthetic materials chemists to tailor and target such properties is greatly hampered by an incomplete knowledge of mechanisms by which zeolites nucleate to form crystals. Amorphous silica nanoparticles are thought to play a key role in the formation of some all-silica zeolites such as silicalite-1.[8,9] Even in this case the atomic-level understanding of critical nucleation and the role of structure-directing agents (SDA) remains quite poor because of the difficulties in characterizing the emergence of atomic-level order at the length scales of zeolite unit cells.[10] In this article, we present an important step toward improving this understanding by showing that a reactive model of silica polymerization and assembly can yield crystalline phases of dense silica, zeolites, and related nanoporous materials.

Several molecular modeling studies have been reported to elucidate the process of zeolite formation.[11] However, relatively few of these simulations actually result in microporous crystalline materials. Deem and co-workers have applied algorithms for predicting hypothetical zeolite structures, resulting in extensive libraries of energetically feasible framework topologies.[12−14] Their approach used a Monte Carlo (MC) procedure to sample positions of Si atoms within a unit cell, followed by insertion of oxygens and energy minimization to yield reasonable structures. Despite this progress, such zeolite discovery algorithms do not follow the actual pathways of zeolite formation.

To address this issue, Jin et al. recently reported an atomic lattice model of silica polymerization on the body-centered cubic (bcc) lattice.[15] Canonical MC simulations of this model reproduce semiquantitative NMR data on the evolution of silica gel formation. In addition, parallel tempering MC simulations of this bcc lattice model yield a wide array of all-silica zeolite analogues as well as layered materials and known chalcogenides. Although this lattice model approach shows promise for revealing qualitative aspects of zeolite nucleation and growth, the use of any lattice model fundamentally limits the possible structures that may form. In particular, no known zeolite topology in the IZA database[16] maps directly onto the bcc lattice. As such, there remains a need for development of an off-lattice model and a sampling algorithm to yield structures of nanoporous crystals such as zeolites.

Malani et al. applied reaction ensemble MC (REMC)[17−19] to sample an off-lattice, spring-tetrahedron model of flexible silica to simulate silica polymerization yielding amorphous gels.[20,21] This work has produced the best agreement to date of any molecular simulation with the evolution of the so-called Q_n distribution—the distribution of silica atoms bound to n

Received: September 26, 2015
Revised: October 30, 2015
Published: November 3, 2015

DOI: 10.1021/acs.jpcc.5b09404
J. Phys. Chem. C 2015, 119, 26628−26635

bridging oxygens—measured by ^{29}Si solid-state NMR. These MC simulations accomplished such agreement through a collection of targeted moves that efficiently capture the fundamental condensation and hydrolysis fluctuations in the formation of silica networks. The same approach was recently applied to model the self-assembly and structures of silica-SDA nanoparticles thought to play a role in silicalite-1 formation.[22]

In this paper we investigate the extent to which this reactive approach to silica polymerization can yield crystalline silica structures, including all-silica zeolite frameworks. Applying molecular simulations to model crystal formation requires methods to surmount free energy barriers that separate disordered and crystalline phases. Replica exchange MC algorithms such as the parallel tempering method[23−27]—simulating several replicas with different temperatures and allowing for replica exchange between MC configurations at adjacent temperatures—have proven useful for equilibrating systems constrained by free energy barriers. Another replica exchange approach developed specifically for reaction ensemble MC was reported by Turner et al.,[28] involving simulations at various values of the appropriate standard free energies of reaction. This method fits naturally within our present silica reaction ensemble model, by simulating system copies with different equilibrium constants controlling silica condensation/hydrolysis reactions. We show below that the replica exchange REMC (RE-REMC) approach promotes ample silica network fluctuations while keeping silica bond lengths and angles within ranges characteristic of a target temperature. As a result, RE-REMC efficiently generates the crystalline ground states of our off-lattice model, producing various dense silica and zeolite crystal structures as confirmed through X-ray pattern analysis. While this means of simulating crystal formation in our model does not follow the pathways encountered in zeolite synthesis because of the nature of the replica-exchange Monte Carlo moves, the results below nevertheless represent an important step by showing that our reactive model of silica assembly can lead to a wide array of dense and nanoporous silica crystals.

The remainder of this article is organized as follows: the next section on sampling and modeling methods describes the model and simulation methods used herein; the following section outlines the replica-exchange Monte Carlo simulations; the subsequent section details the results with discussion for both dense and nanoporous crystal formation; and the last section summarizes the work and offers concluding remarks. We have also included an Appendix with detailed information on the Monte Carlo formulation utilized herein.

SAMPLING AND METHODOLOGIES

Our work makes use of a previously developed molecular model consisting of flexible, corner-sharing tetrahedra to represent silicic acid ($Si(OH)_4$) for silica polymerization.[20,21] Each silica tetrahedron is represented as a hard-sphere core in the center of each tetrahedron with four corners occupied by one of two possible oxygenic species: (i) hydroxyl groups (OH) represented as single particles and/or (ii) bridging oxygen atoms (BO) connecting condensed silica (see Figure 1).

The silica tetrahedron model was proposed by Astala et al. for modeling the mechanical properties of crystalline silica solids.[29] The structure of each flexible tetrahedron is maintained via harmonic springs between BO/OH according to

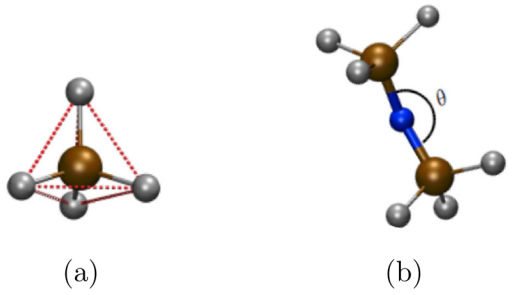

Figure 1. (a) A silica tetrahedral model used in this work. A silicon atom (brown) is in the center of a tetrahedron with hydroxyl groups (gray) are at the vertices. Dashed lines (red) represent the springs between the hydroxyl groups. (b) A silica dimer formed after a condensation reaction. The two silicon atoms are connected through a bridging oxygen (blue) with a Si−O−Si angle (θ).[21]

$$U_1 = \sum_{i=1}^{3} \sum_{j=i+1}^{4} \frac{k_S}{2}(|r_i - r_j| - r_0)^2 \quad (1)$$

where U_1 is the internal potential energy of a tetrahedron, r_i is the position of the ith BO/OH vertex, k_S is a spring constant, and r_0 is the equilibrium distance between two vertices (i.e., oxygen−oxygen distance). The value of k_S was set to 851 kJ mol^{-1} Å^{-2} in our previous work,[30] and r_0 is set to 2.61 Å based on the geometry of silica tetrahedra (Si−O bond length = 1.6 Å and O−Si−O angle = 109.47°).[20,21] A harmonic angular potential applied to the Si−O−Si angle is also included:

$$U_2 = \frac{k_A}{2}(\cos\theta - \cos\theta_0)^2 \quad (2)$$

where θ is the Si−O−Si angle, θ_0 is a reference angle, and k_A is an angular force constant. The value of 155° was used for θ_0 as determined by previous periodic DFT calculations,[30] and the value 226.74 kJ mol^{-1} was used for k_A. A detailed description of the model has been given in previous work.[20−22]

The MC moves included random translations performed on all silica tetrahedra and clusters. In addition, we attempted random translations on terminal hydroxyls (OH) and bridging oxygens (BO), hence producing vibrational excitations of tetrahedra, and eventually rotations from many such atomic translations. These moves were attempted in the canonical ensemble (NVT) to sample important spatial configurations. To sample reaction events leading to silica polymerization in our simulations, REMC was used. REMC eliminates the need for reactive force fields to bring about assembly of the polymerized silica network. The reactive moves include monomer−monomer, monomer−cluster, and cluster−cluster aggregation. These moves were attempted with acceptance probabilities controlled by cluster size through assumed diffusion limitations; intramolecular condensations were attempted via force-bias moves that relax strained ring structures. A detailed description of our implementation of REMC can be found in our recent simulation studies on silica polymerization by Malani et al.[20,21] The attempt probabilities for moves were chosen as 0.97 for translations on all species mentioned above and 0.03 for REMC moves of cluster−cluster and intramolecular reactions.

Replica-Exchange Reaction Ensemble MC (RE-REMC). To allow efficient sampling of the assembly of zeolite structures, we have used a replica exchange reaction ensemble MC (RE-REMC) simulation technique similar to that presented by

DOI: 10.1021/acs.jpcc.5b09404
J. Phys. Chem. C 2015, 119, 26628−26635

Turner et al.[28] In the work of Turner et al., they used the standard Gibbs energy of reaction as a tempering variable, while in this work we use the inverse equilibrium constant, $K_{inv} = K_{eq}^{-1}$, as the tempering variable. Similar to the parallel-tempering MC (PTMC) technique,[23−27] RE-REMC was performed with a number (m) of replicas with each replica having a different inverse hydrolysis reaction equilibrium constant, K_{inv}, in which $K_{inv,1} < K_{inv,2} < K_{inv,3} < ... < K_{inv,m}$. As shown in section S1 of the Supporting Information, the probability of swapping adjacent replicas, m and n, is given by

$$P_{mn} = \min\{1, (\beta P^0 V)_m^{\overline{\nu}(\xi_n-\xi_m)} K_{inv,m}^{\xi_m-\xi_n} (\beta P^0 V)_n^{\overline{\nu}(\xi_m-\xi_n)} K_{inv,n}^{\xi_n-\xi_m}\} \quad (3)$$

Here $\beta = 1/k_B T$ where k_B is Boltzmann's constant and T is absolute temperature; V is volume, and P^0 is the reference pressure that connects an equilibrium constant to a reference free energy; $\overline{\nu} = \sum_i \nu_i$ is the net change in the total number of molecules; and ξ_m and ξ_n are the extents of reaction in the current configuration (before performing a swapping move) in replicas m and n, respectively.

All simulations were initiated with a random configuration in a simulation box of given dimensions, under full three-dimensional periodic boundary conditions. The number of silica tetrahedra and system size were determined by the unit cell parameters of target silica crystals, either dense or zeolitic. We emphasize that setting unit cell parameters does not guarantee that the Monte Carlo simulation will generate fully connected crystal structures. Between 10 and 100 million MC moves were performed to sufficiently complete structural assemblies in each replica. Our use of an off-lattice reactive silica tetrahedron model provides sufficient configurational flexibility to produce a wide array of known crystalline zeolite structures. Such flexibility can also lead to amorphous structures, especially for larger system sizes. With current computational and algorithmic constraints, the system size of 16 tetrahedra represents the maximum we could handle that leads to crystalline materials. In future work, we will push for larger system sizes.

An adequate number of replicas and the choice of $K_{inv,m}$ values are essential to the success of this RE-REMC approach. We have found that using 16 replicas is sufficient for generating silica crystals in our simulations. The grid of $K_{inv,m}$ values began with a minimum value of 10^{-6}, corresponding to a condensation equilibrium constant of 10^6, a value large enough to drive network formation. The rest of the $K_{inv,m}$ values were obtained through the relationship $K_{inv,m+1}/K_{inv,m} = 4$, producing a maximum $K_{inv,16}$ value of 537, sufficient to drive silica hydrolysis and hence network deconstruction and annealing.

For comparison with the RE-REMC results reported below, standard parallel tempering reaction ensemble MC (PT-REMC) was applied, involving the simultaneous simulation of several system replicas, each at a different temperature. The probability of a PT-REMC replica exchange move is given as

$$P_{mn} = \min\{1, \exp[(\beta_m - \beta_n)(U_m - U_n)](\beta P^0 V)_m^{\overline{\nu}(\xi_n-\xi_m)} \times K_{inv,m}^{\xi_m-\xi_n} (\beta P^0 V)_n^{\overline{\nu}(\xi_m-\xi_n)} K_{inv,n}^{\xi_n-\xi_m}\} \quad (4)$$

In the case where $\beta_m = \beta_n$, the PT-REMC probability in eq 4 reverts back to the RE-REMC result in eq 3. The challenge in developing an appropriate, "apples-to-apples" comparison between RE-REMC and PT-REMC is generating a prescription for computing $K_{inv}(T_m)$ values in PT-REMC in agreement with the grid of $K_{inv,m}$ values in RE-REMC. To achieve this, we have assumed that the $K_{inv}(T)$ formula in PT-REMC follows the Arrhenius temperature dependence: $K_{inv}(T) = Ae^{B/RT}$. We emphasize that in the present context these A and B values are posited only to provide a mapping between T_m values in PT-REMC and $K_{inv,m}$ values in RE-REMC; i.e., they may or may not take physically meaningful values. In our mapping approach, we assumed that $A = 537 = K_{inv,max}$ and $B = 12.5$ kJ/mol, a physically reasonable reaction energy for silica hydrolysis.[31] Using these values, we computed a grid of T_m values so that $K_{inv}(T_m)$ (PT-REMC) = $K_{inv,m}$ (RE-REMC), yielding T_m values ranging from 75 to 150 000 K (see Table S2 in Supporting Information for all T_m and $K_{inv,m}$ values).

In general, for both PT-REMC and RE-REMC, replica exchanges were attempted in 10% of moves, with the other 90% of moves being the translations and reaction moves described above. Simulations were performed generally over 100 million MC steps, requiring in the range 1−7 CPU days on 16 2.2 GHz AMD Opteron 848 CPU-cores.

In addition to visualizing the structures obtained, simulated X-ray diffraction (XRD) patterns were computed using the Debyer software (code.google.com/p/debyer/) on systems with 20 × 20 × 20 unit cells to ensure sufficient system size to generate reasonably narrow diffraction peaks. For comparison, XRD patterns were computed using coordinates obtained from the IZA and American Mineralogist Crystal Structure Databases.[16,32]

RESULTS AND DISCUSSION

We now discuss results from RE-REMC simulations on systems with various densities corresponding to different silica polymorphs. Simulations yielding dense silica crystals as well as all-silica zeolite crystals are described below. All materials considered exhibit orthorhombic, tetragonal, or cubic unit cells; the system parameters of all the investigated structures are summarized in Table 1.[16,32]

Table 1. System Parameters of Studied Structures in This Work

structures	no. of SiO_2	box dimensions (Å)
α-cristobalite	16	9.9434 × 9.9434 × 6.922
β-cristobalite	8	7.16 × 7.16 × 7.16
keatite	12	7.46 × 7.46 × 8.61
SOD	12	8.9561 × 8.9561 × 8.9561
ATT	12	9.980 × 7.514 × 9.369
DFT	8	7.075 × 7.075 × 9.023
EDI	5	6.926 × 6.926 × 6.410

Formation of Dense Silica Polymorphs. To test the RE-REMC sampling technique, we started our investigation with a random initial condition of 8 tetrahedra in a box whose dimensions match the density of β-cristobalite, a high temperature and low pressure polymorph of silica. REMC without replica exchange was not found to yield any crystalline structure. In contrast, REMC with replica exchange as outlined above with various equilibrium constants was found to yield a fully condensed crystal of β-cristobalite in the first replica (with $K_{inv} = 10^{-6}$) after 4 million MC steps (see Figure 2). The XRD patterns of RE-REMC-simulated and known β-cristobalite crystals[32] are shown to agree very well in Figure 3.

We then applied RE-REMC to study silica polymerization in a box with density corresponding to that of α-cristobalite. This

DOI: 10.1021/acs.jpcc.5b09404
J. Phys. Chem. C 2015, 119, 26628−26635

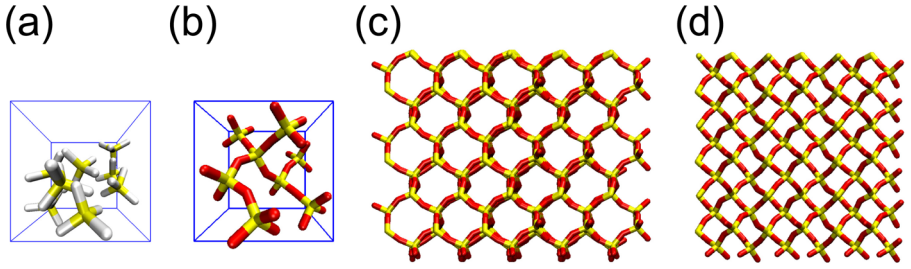

Figure 2. Snapshots of (a) initial configuration, (b) final structure, and (c, d) two orthographic views of a 3 × 3 × 3 extension of the configuration of β-cristobalite obtained from the RE-REMC simulation. Color code: Si (yellow), bridging oxygen (red), hydroxyl group (white).

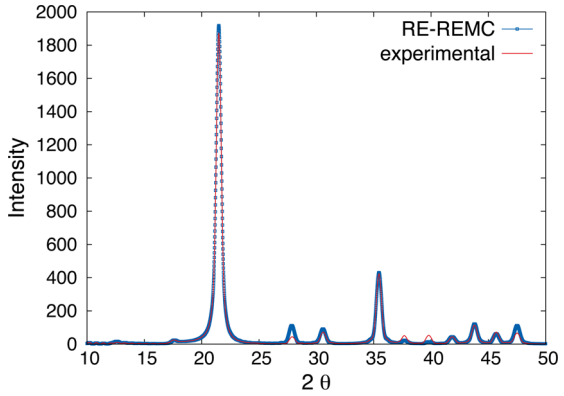

Figure 3. Calculated XRD patterns for β-cristobalite comparing RE-REMC structures and known coordinates from experimental XRD.

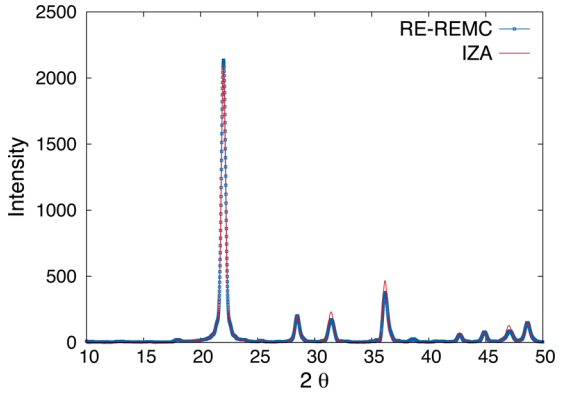

Figure 5. Calculated XRD patterns for α-cristobalite comparing RE-REMC structures and known coordinates from experimental XRD.

represents the largest simulation cell that we studied, with 4 unit cells containing a total of 16 silica tetrahedra in a box of dimension 9.9434 Å × 9.9434 Å × 6.922 Å. α-Cristobalite crystals formed in RE-REMC after 55 million RE-REMC steps. Figure 4 shows the visualizations of initial and final configurations of the obtained results on α-cristobalite simulations. The XRD patterns of simulated and known α-cristobalite structures are shown in Figure 5.

We also applied RE-REMC to study silica polymerization in a system with density corresponding to that of crystalline keatite, a silica polymorph with density higher than those of β-cristobalite and α-cristobalite. Crystalline keatite was found in the first replica (with $K_{inv} = 10^{-6}$) in 4.5 million MC steps; the XRD patterns of simulated and known keatite are shown in Figure S3. It is instructive to point out that the MC simulations without replica exchange moves did not produce crystalline keatite, even after 26 million MC steps with K_{inv} of 10^{-6}. This suggests that configuration exchange between adjacent replicas strongly increases the likelihood of overcoming energy barriers between amorphous and keatite phases.

Having established the utility of the RE-REMC approach for generating silica crystals, we now compare this with the PT-REMC method using the temperature mapping discussed above. Using the initial condition that generated β-cristobalite with the RE-REMC method, we applied PT-REMC with the temperature mapping involving temperatures in the range 75–150 000 K (see Table S2). We found that PT-REMC also produced crystalline β-cristobalite after 4 million MC steps. The PT-REMC replicas with the lowest three temperatures (75, 80, and 87 K) were found to produce crystalline β-cristobalite. For comparison, the RE-REMC replicas with the lowest *five* values of K_{inv} were found to crystallize β-cristobalite. In addition, high temperature replicas in PT-REMC produced rather distorted silica tetrahedra that are not representative of structures found in silica materials. Finally, replica exchange probabilities were of order 10^{-2} in RE-REMC, but only of order 10^{-4} in PT-REMC. For these reasons, we conducted the remainder of our study using the RE-REMC approach.

Formation of All-Silica Zeolite Frameworks. Sodalite (SOD) is a porous aluminosilicate material with ultrasmall cages and windows accessible only to small molecules such as

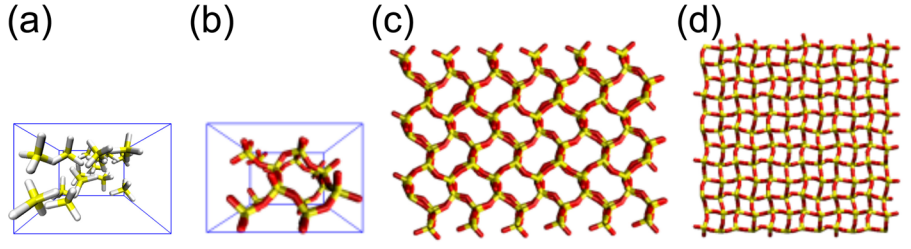

Figure 4. Snapshots of (a) initial configuration, (b) final structure, and (c, d) two orthographic views of a 3 × 3 × 3 extension of the configuration of α-cristobalite obtained from the RE-REMC simulation. Color code: Si (yellow), bridging oxygen (red), hydroxyl group (white).

DOI: 10.1021/acs.jpcc.5b09404
J. Phys. Chem. C 2015, 119, 26628–26635

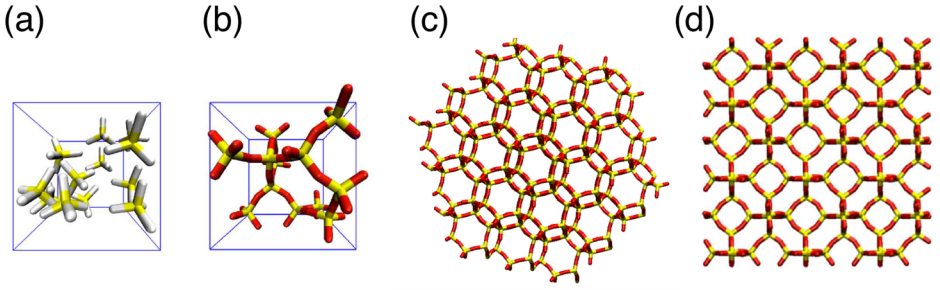

Figure 6. Snapshots of (a) initial configuration, (b) final structure, and (c, d) two orthographic views of a 3 × 3 × 3 extension of the SOD configuration obtained from the RE-REMC simulation. Color code: Si (yellow), bridging oxygen (red), hydroxyl group (white).

water. The all-silica SOD was synthesized for the first time several decades ago.[33] We applied RE-REMC to study silica polymerization for a system with density corresponding to that of all-silica SOD, by beginning with an initially random collection of 12 silica tetrahedra in the appropriately sized box (see Table 1). A fully condensed crystal with the SOD framework structure was obtained in the first replica after 3.3 million RE-REMC steps. The initial and final configurations are shown in Figures 6a and 6b, respectively. Small sodalite cages and windows can also be seen in the 3 × 3 × 3 periodic extension of the final configuration, shown in Figures 6c and 6d.

Figure 7 shows the calculated XRD pattern of the simulated SOD crystal structure from RE-REMC for comparison with the

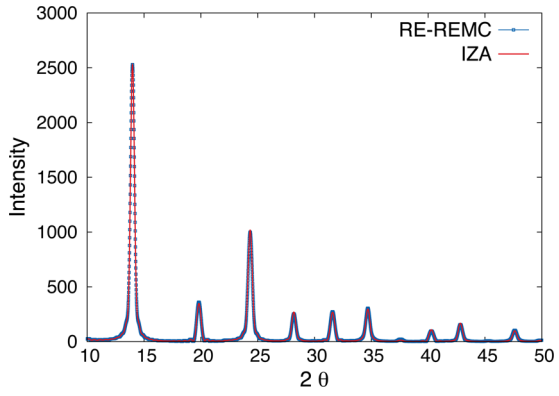

Figure 7. Calculated XRD patterns for SOD comparing RE-REMC structures and known coordinates from the IZA database.

XRD pattern computed from the known SOD structure.[16] The striking agreement shown in Figure 7 shows the quantitative agreement in crystal structure arising from the RE-REMC simulation.

Next we simulated silica polymerization in a system box with density corresponding to the all-silica EDI zeolite—a small-pore zeolite whose tetragonal unit cell consists of five TO_2 (T = Al or Si) units. Despite the fact that to our knowledge an all-silica version of EDI zeolite has not yet been synthesized, EDI remains a promising target for our RE-REMC approach because of its relatively small unit cell. The RE-REMC simulation initiated with random configurations in each replica using the corresponding dimensions in Table 1 and formed EDI crystals after 3 million RE-REMC steps. The atomic structure obtained from our RE-REMC can be seen in Figure 8. The XRD patterns of simulated and known EDI, shown in Figure 9, demonstrate again quantitative agreement between known EDI structure and RE-REMC results.

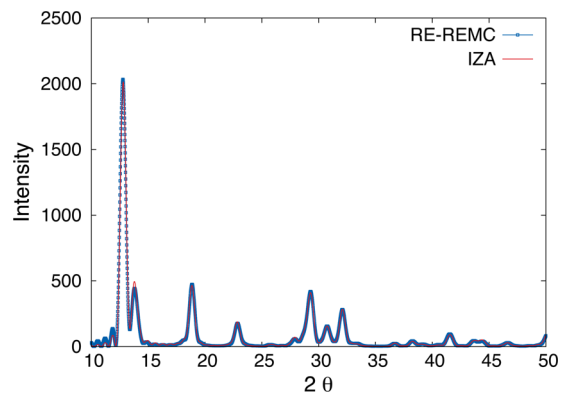

Figure 9. Calculated XRD patterns for EDI framework comparing RE-REMC structures and known coordinates from experimental XRD.

Nonsilica-based materials may also provide targets for our tetrahedral RE-REMC approach. The open-framework cobalt phosphate material with DFT structure[34] was studied with our RE-REMC approach. Crystals of DFT were formed in our

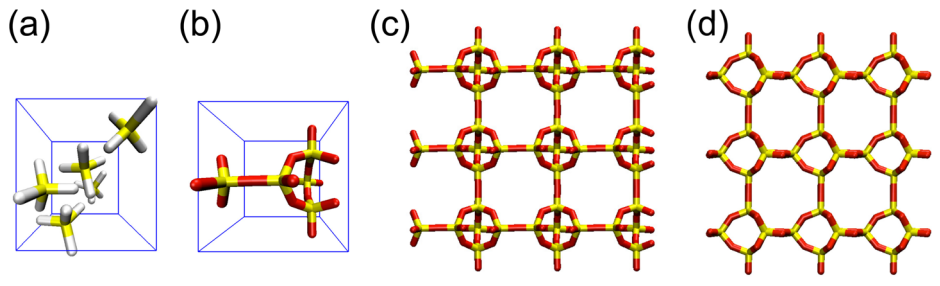

Figure 8. Snapshots of (a) initial configuration, (b) final structure, and (c, d) two orthographic views of a 3 × 3 × 3 extension of the configuration of EDI obtained from the RE-REMC simulation. Color code: Si (yellow), bridging oxygen (red), hydroxyl group (white).

DOI: 10.1021/acs.jpcc.5b09404
J. Phys. Chem. C 2015, 119, 26628−26635

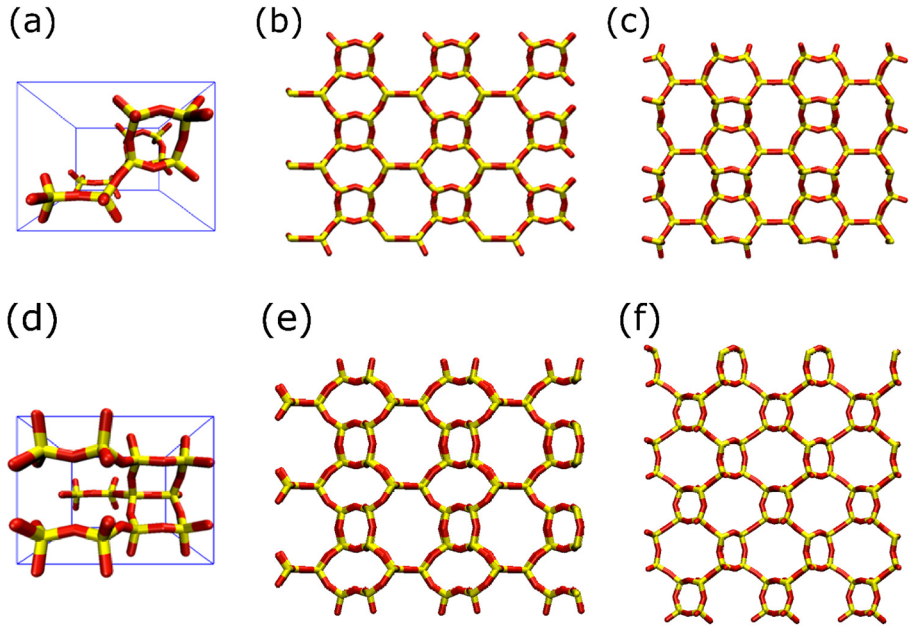

Figure 10. Snapshots of (a) final structure and (b, c) two orthographic views of the final structure with 3 × 3 × 3 extension obtained in RE-REMC *replica 1* with the ATT lattice parameter; (d), (e), (f) same as (a), (b), (c) except from RE-REMC *replica 2*. Color code: Si (yellow), bridging oxygen (red).

simulation after 4 million steps, giving rise to the XRD pattern shown in Figure S4, again in quantitative agreement with the IZA database. We find it most interesting that a model based on silica tetrahedra can produce crystals of a material composed of cobalt phosphate, $Co_3(PO_4)_2$.

We also applied our tetrahedral REMC approach to simulate polymerization among tetrahedra at the density of ATT, an aluminophosphate (AlPO) material. Fully connected structures were obtained after 50 million RE-REMC steps in the first two replicas. Interestingly, in the case of the ATT study, these two replicas produced slightly different structures as shown in Figure10. We have also calculated the energies of the two structures. The known ATT framework has energy of 90.8 kJ/mol per unit cell within our model, whereas the second predicted structure has energy of 173.3 kJ/mol per unit cell. The contribution of the energy difference between the two structures mostly comes from the angular potential. Angles deviate more from the reference angle of the tetrahedral model in the predicted structure. The angular potential of the obtained ATT framework is 84.2 kJ/mol, and that of our predicted structure is 166.7 kJ/mol. This result suggests that the previously known structure of ATT is the more stable one from an energetic point of view.

To examine these different crystal structures, we computed their XRD patterns. The upper part of Figure 11 shows that the structure obtained from the second replica exhibits the known ATT framework structure, whereas the structure obtained from the first replica does not. This shows how subtle changes in crystal structure manifest clearly in computed XRD patterns. However, the lower part of Figure 11 shows that the structure from replica 1 agrees well with the predicted silica-based structure PCOD 3102553 (from Predicted Crystallography Open Database) by Le Bail.[35] It can be seen that the major XRD peaks of these two structures are well aligned with only small shifts. This finding also suggests that our tetrahedral model can also predict different crystalline zeolite structures which have not been fabricated yet.

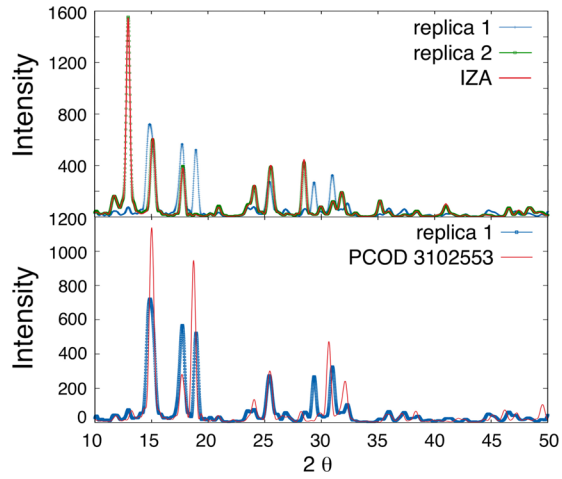

Figure 11. Upper: calculated XRD patterns comparing ATT framework obtained from IZA Web site and RE-REMC *replicas 1* and 2. Lower: calculated XRD patterns comparing the predicted structure from GRINSP 2.00 (PCOD 3102553)[35] and obtained from RE-REMC *replica 1*.

Given that our RE-REMC approach with a tetrahedral model based on silica polymerization can generate structures of an open framework cobalt phosphate, DFT, and an AlPO material, ATT zeolite, it is worthwhile to speculate about why this is the case. The two frameworks involve corner-sharing tetrahedra, in which Al−O bond lengths are in the range 1.70−1.75 Å, while P−O bond lengths are 1.50−1.58 Å.[36−38] Averaging these ranges yields 1.6 Å, close to the Si−O bond length in our model,[29] which explains why this silica tetrahedral model also fairly well reproduces XRD patterns for Co-phosphates and AlPOs.

SUMMARY AND CONCLUSIONS

In summary, we have applied a replica-exchange reaction ensemble MC (RE-REMC) approach to search for ground state

DOI: 10.1021/acs.jpcc.5b09404
J. Phys. Chem. C 2015, 119, 26628−26635

structures of several open-framework materials, including all-silica zeolites and related cobalt phosphate and aluminophosphate materials. Our approach is based on three-dimensional polymerization of semirigid tetrahedral units undergoing condensation/hydrolysis chemistry in the reaction ensemble. This reactive model was previously used to model the formation of amorphous silica gels and silica nanoparticles, and results shown very good agreement with the experimental observations. With the replica exchange, this approach has produced crystals of dense silica polymorphs α-cristobalite, β-cristobalite, and keatite as well as crystals of open-framework materials with SOD, EDI, DFT, and ATT structures, confirmed by computing XRD patterns for comparison with known coordinates. Future RE-REMC studies of our tetrahedral model may involve simulating at constant pressure with volume fluctuations to determine how changing pressure can influence the resulting crystalline structures.

The behavior of our off-lattice silica polymerization model, as shown by the crystal structures formed above, augurs well for the application of this model in future work to simulate the crystallization pathways followed when forming these materials. Doing so would require using sampling approaches different from replica exchange Monte Carlo, which avoids free energy barriers through replica exchange. Methods for sampling free energy barriers characterized by collective order parameters (i.e., reaction coordinates) will be required to elucidate the kinetics of crystallization.[39] Nonetheless, this work is important in showing that our model of reactive silica assembly can indeed generate crystalline silica structures, including all-silica zeolites. Our modeling approach opens the door to more detailed understanding of the kinetics and mechanisms of zeolite crystallization for both all-silica and non-silica-based open-framework materials.

APPENDIX

A1. Probability of Replica-Exchange Monte Carlo Moves

In the reaction system studied herein, A + B → C + D, the sum of the stoichiometric coefficients, $\bar{\nu}$, equals zero. Accordingly, the acceptance probability provided in eq 3 becomes

$$P_{mn} = \min\{1, K_{\mathrm{inv},m}^{\xi_m-\xi_n} K_{\mathrm{inv},n}^{\xi_n-\xi_m}\} \tag{5}$$

Furthermore, the quantities, $\xi_n - \xi_m = N_{\mathrm{BO}n} - N_{\mathrm{BO}m}$, in which $N_{\mathrm{BO}m}$ and $N_{\mathrm{BO}n}$ are the numbers of bridging oxygens in replica m and n, respectively. Accordingly, the final form of the RE-REMC probability with K_{inv} ($K_{\mathrm{inv}} = 1/K_{\mathrm{eq}}$) can be used herein:

$$P_{mn} = \min\left\{1, \left(\frac{K_{\mathrm{inv},n}}{K_{\mathrm{inv},m}}\right)^{\xi_n-\xi_m}\right\} = \min\left\{1, \left(\frac{K_{\mathrm{inv},n}}{K_{\mathrm{inv},m}}\right)^{N_{\mathrm{BO}n}-N_{\mathrm{BO}m}}\right\} \tag{6}$$

A2. Simulation Algorithm

To implement the RE-REMC, 16 replicas were used with different inverse equilibrium constants, K_{inv}, ranging from 10^{-6} to 536.87 with ratio of $K_{\mathrm{inv},m+1}$ to $K_{\mathrm{inv},m}$ of 4. Lower K_{inv} values facilitate the search for ground state structures, whereas higher K_{inv} values increase the likelihood of crossing energy barriers between local energy minima.

The probability for conventional Monte Carlo moves, P_{MC}, was set to 0.9, for sufficient sampling of possible configurations with a given equilibrium constant, while the probability for replica exchange moves, P_{RE}, was set to 0.1, for crossing energy barriers between replicas.

The simulation was implemented as follows: Pick a move between replica exchange and conventional Monte Carlo using a random number. If the random number is smaller than P_{MC}, conventional Monte Carlo move is performed in all replicas. If the random number is greater than P_{MC}, the replica exchange move is carried out as following:

- Using random number to pick a replica, m (the inverse equilibrium constant is $K_{\mathrm{inv},m}$). And then m + 1 replica (the inverse equilibrium constant is $K_{\mathrm{inv},m+1}$) is chosen for exchange.
- Determine the numbers of bridging oxygen generated from those two replicas, $N_{\mathrm{BO}m}$ in replica m and $N_{\mathrm{BO}m+1}$ in replica m + 1, respectively.
- Calculate the probability of replica exchange between replica m and replica m + 1 by using eq 6.

ASSOCIATED CONTENT

Supporting Information

The Supporting Information is available free of charge on the ACS Publications website at DOI: 10.1021/acs.jpcc.5b09404.

Section S1; Table S2, and Figures S3 and S4 (PDF)

AUTHOR INFORMATION

Corresponding Authors

*E-mail: auerbach@chem.umass.edu (S.M.A.).
*E-mail: monson@ecs.umass.edu (P.A.M.).

Notes

The authors declare no competing financial interest.

ACKNOWLEDGMENTS

This work was supported by a grant from the U.S. Department of Energy (Contract DE-FG02-07ER46466). We also acknowledge computational resources provided by the Massachusetts Green High-Performance Computing Center (MGHPCC).

REFERENCES

(1) Corma, A. From Microporous to Mesoporous Molecular Sieve Materials and Their Use in Catalysis. *Chem. Rev.* **1997**, *97*, 2373−2420.
(2) Yang, P.; Deng, T.; Zhao, D.; Feng, P.; Pine, D.; Chmelka, B. F.; Whitesides, G. M.; Stucky, G. D. Hierarchically Ordered Oxides. *Science* **1998**, *282*, 2244−2246.
(3) Valtchev, V.; Tosheva, L. Porous Nanosized Particles: Preparation, Properties, and Applications. *Chem. Rev.* **2013**, *113*, 6734−6760.
(4) Davis, M. E. Zeolites from a Materials Chemistry Perspective. *Chem. Mater.* **2014**, *26*, 239−245.
(5) Seo, Y.; Lee, S.; Jo, C.; Ryoo, R. Microporous Aluminophosphate Nanosheets and Their Nanomorphic Zeolite Analogues Tailored by Hierarchical Structure-Directing Amines. *J. Am. Chem. Soc.* **2013**, *135*, 8806−8809.
(6) Moliner, M.; Rey, F.; Corma, A. Towards the Rational Design of Efficient Organic Structure-Directing Agents for Zeolite Synthesis. *Angew. Chem., Int. Ed.* **2013**, *52*, 13880−13889.
(7) Rimer, J. D.; Kumar, M.; Li, R.; Lupulescu, A. I.; Oleksiak, M. D. Tailoring the Physicochemical Properties of Zeolite Catalysts. *Catal. Sci. Technol.* **2014**, *4*, 3762−3771.
(8) Corma, A.; Davis, M. E. Issues in the Synthesis of Crystalline Molecular Sieves: Towards the Crystallization of Low Framework-Density Structures. *ChemPhysChem* **2004**, *5*, 304−313.
(9) Auerbach, S. M.; Fan, W.; Monson, P. A. Modelling the Assembly of Nanoporous Silica Materials. *Int. Rev. Phys. Chem.* **2015**, *34*, 35−70.
(10) Auerbach, S. M.; Ford, M. H.; Monson, P. New Insights into Zeolite Formation from Molecular Modeling. *Curr. Opin. Colloid Interface Sci.* **2005**, *10*, 220−225.

DOI: 10.1021/acs.jpcc.5b09404
J. Phys. Chem. C 2015, 119, 26628−26635

(11) Schmidt, J. E.; Deem, M. W.; Davis, M. E. Synthesis of a Specified, Silica Molecular Sieve by Using Computationally Predicted Organic Structure-Directing Agents. *Angew. Chem., Int. Ed.* **2014**, *53*, 8372−8374.
(12) Falcioni, M.; Deem, M. W. A Biased Monte Carlo Scheme for Zeolite Structure Solution. *J. Chem. Phys.* **1999**, *110*, 1754−1766.
(13) Earl, D. J.; Deem, M. W. Toward a Database of Hypothetical Zeolite Structures. *Ind. Eng. Chem. Res.* **2006**, *45*, 5449−5454.
(14) Pophale, R.; Cheeseman, P. A.; Deem, M. W. A Database of New Zeolite-Like Materials. *Phys. Chem. Chem. Phys.* **2011**, *13*, 12407−12412.
(15) Jin, L.; Auerbach, S. M.; Monson, P. A. Emergence of Zeolite Analogs and Other Microporous Crystals in an Atomic Lattice Model of Silica and Related Materials. *J. Phys. Chem. Lett.* **2012**, *3*, 761−765.
(16) Baerlocher, C.; McCusker, L. B.; Olson, D. H. *Atlas of Zeolite Framework Types*, 6th ed.; Elsevier: Amsterdam, 2007.
(17) Johnson, J. K.; Panagiotopoulos, A. Z.; Gubbins, K. E. Reactive Canonical Monte Carlo: A New Simulation Technique for Reacting or Associating Fluids. *Mol. Phys.* **1994**, *81*, 717−733.
(18) Smith, W. R.; Triska, B. The Reaction Ensemble Method for the Computer Simulation of Chemical and Phase Equilibria. I. Theory and Basic Examples. *J. Chem. Phys.* **1994**, *100*, 3019−3027.
(19) Turner, C. H.; Brennan, J. K.; Lísal, M.; Smith, W. R.; Karl Johnson, J.; Gubbins, K. E. Simulation of Chemical Reaction Equilibria by the Reaction Ensemble Monte Carlo Method: A Review. *Mol. Simul.* **2008**, *34*, 119−146.
(20) Malani, A.; Auerbach, S. M.; Monson, P. A. Probing the Mechanism of Silica Polymerization at Ambient Temperatures Using Monte Carlo Simulations. *J. Phys. Chem. Lett.* **2010**, *1*, 3219−3224.
(21) Malani, A.; Auerbach, S. M.; Monson, P. A. Monte Carlo Simulations of Silica Polymerization and Network Formation. *J. Phys. Chem. C* **2011**, *115*, 15988−16000.
(22) Chien, S.-C.; Auerbach, S. M.; Monson, P. A. Modeling the Self-Assembly of Silica-Templated Nanoparticles in the Initial Stages of Zeolite Formation. *Langmuir* **2015**, *31*, 4940−4949.
(23) Swendsen, R. H.; Wang, J.-S. Replica Monte Carlo Simulation of Spin-Glasses. *Phys. Rev. Lett.* **1986**, *57*, 2607−2609.
(24) Kofke, D. A. On the Acceptance Probability of Replica-Exchange Monte Carlo Trials. *J. Chem. Phys.* **2002**, *117*, 6911−6914.
(25) Kone, A.; Kofke, D. A. Selection of Temperature Intervals for Parallel-Tempering Simulations. *J. Chem. Phys.* **2005**, *122*, 206101.
(26) Rathore, N.; Chopra, M.; de Pablo, J. J. Optimal Allocation of Replicas in Parallel Tempering Simulations. *J. Chem. Phys.* **2005**, *122*, 024111.
(27) Earl, D. J.; Deem, M. W. Parallel Tempering: Theory, Applications, and New Perspectives. *Phys. Chem. Chem. Phys.* **2005**, *7*, 3910−3916.
(28) Turner, C. H.; Brennan, J. K.; Lisal, M. Replica Exchange for Reactive Monte Carlo Simulations. *J. Phys. Chem. C* **2007**, *111*, 15706−15715.
(29) Astala, R.; Auerbach, S. M.; Monson, P. A. Normal Mode Approach for Predicting the Mechanical Properties of Solids from First Principles: Application to Compressibility and Thermal Expansion of Zeolites. *Phys. Rev. B: Condens. Matter Mater. Phys.* **2005**, *71*, 014112.
(30) Astala, R.; Auerbach, S. M.; Monson, P. A. Density Functional Theory Study of Silica Zeolite Structures: Stabilities and Mechanical Properties of SOD, LTA, CHA, MOR, and MFI. *J. Phys. Chem. B* **2004**, *108*, 9208−9215.
(31) Mora-Fonz, M. J.; Catlow, C. R. A.; Lewis, D. W. Oligomerization and Cyclization Processes in the Nucleation of Microporous Silicas. *Angew. Chem.* **2005**, *117*, 3142−3146.
(32) Downs, R.; Hall-Wallace, M. The American Mineralogist Crystal Structure Database. *Am. Mineral.* **2003**, *88*, 247−250.
(33) Bibby, D. M.; Dale, M. P. Synthesis of Silica-Sodalite from Non-aqueous Systems. *Nature* **1985**, *317*, 157−158.
(34) Chen, J.; Natarajan, S.; Thomas, J. M.; Jones, R. H.; Hursthouse, M. B. A Novel Open-Framework Cobalt Phosphate Containing a Tetrahedrally Coordinated Cobalt(II) Center: CoPO4 0.5 C2H10N2. *Angew. Chem., Int. Ed. Engl.* **1994**, *33*, 639−640.
(35) Le Bail, A. Inorganic Structure Prediction with *GRINSP*. *J. Appl. Crystallogr.* **2005**, *38*, 389−395.
(36) Smith, J. V.; Bailey, S. W. Second Review of Al−O and Si−O Tetrahedral Distances. *Acta Crystallogr.* **1963**, *16*, 801−811.
(37) Bnown, G. E.; Gibbs, G. V.; Ribbe, P. H. The Nature and the Variation in Length of the Si-O-Si and Al-O Bonds in Framework of Silicates. *Am. Mineral.* **1969**, *54*, 1044−1061.
(38) Popović, D. d. W.; Boeyens, J. C. A. Correlation between Raman Wavenumbers and P-O Bond Lengths in Crystalline Inorganic Phosphates. *J. Raman Spectrosc.* **2005**, *36*, 2−11.
(39) Allen, R. J.; Valeriani, C.; ten Wolde, P. R. Forward Flux Sampling for Rare Event Simulations. *J. Phys.: Condens. Matter* **2009**, *21*, 463102.

DOI: 10.1021/acs.jpcc.5b09404
J. Phys. Chem. C 2015, 119, 26628−26635